EDGEWOOD

CHEMICAL BIOLOGICAL CENTER

U.S. ARMY RESEARCH, DEVELOPMENT AND ENGINEERING COMMAND

ECBC-CR-102

BIOLOGICALLY INSPIRED POLYMER MICROFIBRILLAR ARRAYS FOR MASK SEALING

Eugene Cheung
Burak Aksak
Metin Sitti

CARNEGIE MELLON UNIVERSITY
Pittsburgh, PA 15213

April 2009

ABERDEEN PROVING GROUND, MD 21010-5424

Disclaimer

The findings in this report are not to be construed as an official Department of the Army position unless so designated by other authorizing documents.

REPORT DOCUMENTATION PAGE

Form Approved
OMB No. 0704-0188

1. REPORT DATE *(DD-MM-YYYY)*	2. REPORT TYPE	3. DATES COVERED *(From - To)*
XX-04-2009	Final	May 2008 - Nov 2008

4. TITLE AND SUBTITLE
Biologically Inspired Polymer Microfibrillar Arrays for Mask Sealing

5a. CONTRACT NUMBER
W911NF-07-D-0001

5b. GRANT NUMBER

5c. PROGRAM ELEMENT NUMBER

6. AUTHOR(S)
Cheung, Eugene; Aksak, Burak; and Sitti, Metin (Carnegie Mellon University)

5d. PROJECT NUMBER
DTRA 8R22GA

5e. TASK NUMBER
TCN 07090

5f. WORK UNIT NUMBER

7. PERFORMING ORGANIZATION NAME(S) AND ADDRESS(ES)
Carnegie Mellon University, 5000 Forbes Ave., Pittsburgh, PA 15213

8. PERFORMING ORGANIZATION REPORT NUMBER
ECBC-CR-102

9. SPONSORING / MONITORING AGENCY NAME(S) AND ADDRESS(ES)
U.S. Army Research Office, P.O. Box 12211, Research Triangle Park, NC 27709
Defense Threat Reduction Agency, 8725 John J. Kingman Road, Fort Belvoir, VA 22060-6201

10. SPONSOR/MONITOR'S ACRONYM(S)
ARO
DTRA

11. SPONSOR/MONITOR'S REPORT NUMBER(S)

12. DISTRIBUTION / AVAILABILITY STATEMENT
Approved for public release; distribution is unlimited.

13. SUPPLEMENTARY NOTES
COR: Karen M. Coyne, AMSRD-ECB-RT-PR, (410) 436-6520

14. ABSTRACT
Previous work to develop a microfibrillar array to improve mask sealing performance demonstrated increased wet and dry adhesion on rigid and soft smooth substrates using spatulate fibers. The current effort modeled and characterized dry fibrillar adhesion to substrates that more closely approximate human skin. The models for adhesion to soft, textured substrates revealed that the resulting adhesion was simply a fraction of the adhesion to a smooth, rigid substrate. The exact fraction depends on the fiber and substrate properties. The addition of a water layer further reduced the adhesion. Friction performance was shown to directly follow adhesion performance. More research is required to optimize the adhesives to improve mask sealing. Surface coatings on the fibers are one possibility for increasing adhesion to human skin.

15. SUBJECT TERMS

Biologically inspired adhesion	Fibrillar adhesion	Gecko adhesion
Mask sealing	Face masks	Adhesion

16. SECURITY CLASSIFICATION OF:			17. LIMITATION OF ABSTRACT	18. NUMBER OF PAGES	19a. NAME OF RESPONSIBLE PERSON
a. REPORT	b. ABSTRACT	c. THIS PAGE			Sandra J. Johnson
U	U	U	UL	19	19b. TELEPHONE NUMBER *(include area code)* (410) 436-2914

Blank

PREFACE

The work described in this report was authorized under Contract No. W911NF-07-D-0001. The Task was performed under a Scientific Services Agreement issued by Battelle Chapel Hill Operations, 50101 Governors Drive, Suite 110, Chapel Hill, NC. This work was supported by the Defense Threat Reduction Agency Project No. 8R22GA under the auspices of the U.S. Army Research Office Scientific Services Program administered by Battelle (Delivery Order 0068). This work was started in May 2008 and completed in November 2008.

BLANK

CONTENTS

1. INTRODUCTION 7

2. MODELING OF BIOLOGICALLY INSPIRED ADHESIVES 7

3. ADHESIVE FABRICATION 10

3.1 Microfibers 10
3.2 Substrates 11

4. TENSILE ADHESION TESTS 12

4.1 Tensile Adhesion Measurement Setup 12
4.2 Soft Substrate Adhesion Results and Discussion 12
4.2.1 Smooth Soft Substrates 12
4.2.2 Textured Soft Substrates 14
4.2.3 Water Covered Soft Textured Substrates 14

5. FRICTION TESTS ON SOFT SUBSTRATES 16

6. SEALING TESTS 18

7. CONCLUSIONS 18

LITERATURE CITED 19

FIGURES

1. Normalized pull-off force for varying β 9

2. Model simulations examining the effect of changing the fiber radius and fiber material modulus 10

3. Top view microscope images of fibers with spatulate tips fabricated on acrylic pegs 11

4. Sketch of the measurement setup used to perform flat-flat tensile adhesion tests with fibers fabricated on the end of an acrylic peg. 12

5. Compiled results of the smooth soft substrate adhesion tests 13

6. Compiled results of the textured soft substrate adhesion tests 15

7. Results of adhesion tests on textured soft substrates with a thin water layer 15

8. Results of friction tests on textured soft substrates 17

BIOLOGICALLY INSPIRED POLYMER MICROFIBRILLAR ARRAYS FOR MASK SEALING

1. INTRODUCTION

The U.S. Army Edgewood Chemical Biological Center is investigating novel sealing technologies for respiratory protective masks to address current shortfalls in operational performance due to improper fitting and donning practices. One promising area is biologically inspired dry adhesives. Geckos, spiders, beetles, flies, and many other climbing lizards and insects have a variety of sub-millimeter scale fibers on their feet to robustly and efficiently climb on a wide range of smooth and rough surfaces. These micro/nano structures enable strong, robust, and repeatable adhesion and friction in addition to being self-cleaning of dirt and other contaminants on surfaces. This work aims to investigate the usage of a synthetic version of these fibrillar adhesion mechanisms in improving mask sealing performance.

In Phases I and II,[1] much progress was made toward the use of biologically inspired micro-fibrillar arrays for the improvement of mask sealing performance. Approximate models of dry and wet adhesion on smooth surfaces were developed and experimentally verified. Fabricated synthetic adhesives with spatulate tips demonstrated pronounced adhesion enhancements on smooth substrates (both rigid and soft). Adhesion tests on textured soft synthetic surfaces suggested minimization of the microfiber diameter to optimize adhesion. Furthermore, the addition of a thin oil layer was found to enhance adhesion only slightly, and the added complications that come with this option led to the decision to concentrate on dry adhesives. Sealing tests revealed that the microfibers on their own are incapable of maintaining a seal, but the simple addition of a sealing structure results in a capable sealant.

The work in Phase III concentrated on modeling and characterizing dry fibrillar adhesion to substrates that more closely approximate the target application of human facial skin.

2. MODELING OF BIOLOGICALLY INSPIRED ADHESIVES

Work done in Phase II[1] showed that fibers with spatulate tips were capable of greatly enhancing adhesion to soft substrates. However, the previously developed models cannot accurately describe the overall adhesion of a fiber array to these soft substrates. The deformation of the substrate as the fibers pull off couples the adhesion of neighboring fibers resulting in a decrease in adhesion, an effect that was not captured in the old models.

Fortunately, recent work done by this lab in collaboration with Professor Chung-Yuen Hui at Cornell University provides a solution. In a paper published in the *Journal of Applied Physics*, a model was developed to describe the effect of backing layer thickness on the adhesion of fibrillar arrays.[2] The numerical model describes the adhesion between a rigid cylindrical punch contacting an array of microfibers with an elastic backing layer. This scenario is nearly identical to an array of fibers on a cylindrical punch (with no backing layer) contacting an elastic soft substrate. The only difference is the interface that separates during pull-off: in the

paper, the fibers separate from the rigid punch; for this work, the fibers separate from the soft substrate. This difference is immaterial to the analysis (it is important to ensure that the correct interface separates, but this is trivial), and thus the equations can be used with no alterations.

The normalized pull-off force was found to depend on a single dimensionless parameter β:

$$\bar{F}_p = \frac{2}{\pi\sqrt{\beta}}, \tag{1}$$

The dimensionless parameter β is a function of the material and geometrical properties of the substrate and fibers:

$$\beta = \frac{4}{\pi^2}\bar{C}_{f\infty}(\alpha^*) - \frac{2}{\pi^2}\alpha^*\bar{C}'_{f\infty}(\alpha^*)\left[1 - \frac{\chi'(\eta)\eta}{1+\chi(\eta)}\right], \tag{2}$$

where

$$\bar{C}_{f\infty}(\alpha^*) = \frac{\pi^2(\alpha^*)^2 + 46.4\alpha^* + 16}{4\alpha^* + 16}, \tag{3}$$

$$\alpha^* = \frac{ka}{2\pi G[1+\chi(\eta)]}, \tag{4}$$

$$\chi(\eta) = \frac{1.095\eta + 1.3271\eta^2 + 0.1431\eta^3}{0.9717}, \tag{5}$$

$$\eta = \frac{a}{h}. \tag{6}$$

In the above equations, a is the radius of the fiber array, h is the thickness of the substrate, k is the stiffness of the fiber array, and G is the shear modulus of the substrate material. The fiber array stiffness k can be calculated as

$$k = \rho k_f = \frac{\rho E_f A}{L}, \tag{7}$$

where ρ is the number of fibers per unit area, k_f is the stiffness of a single fiber, E_f is the Young's modulus of the fiber material, A is the cross section of a single fiber, and L is the length of a single fiber. Direct evaluation reveals that the minimum value of β is $4/\pi^2 \approx 0.4$.

It is important to note that these equations are a fit to numerical finite element results. The results of eq 1 and the numerical simulations can be seen in Figure 1. Clearly the equation and simulations are in excellent agreement. It can also be seen that the effect of a soft substrate can only decrease adhesion. Furthermore, the decrease is quite rapid for small β, but becomes less pronounced for larger β. It should be noted that a larger β corresponds to a more compliant substrate (softer and thicker). For the application of human facial skin, the target β will certainly be in the larger range.

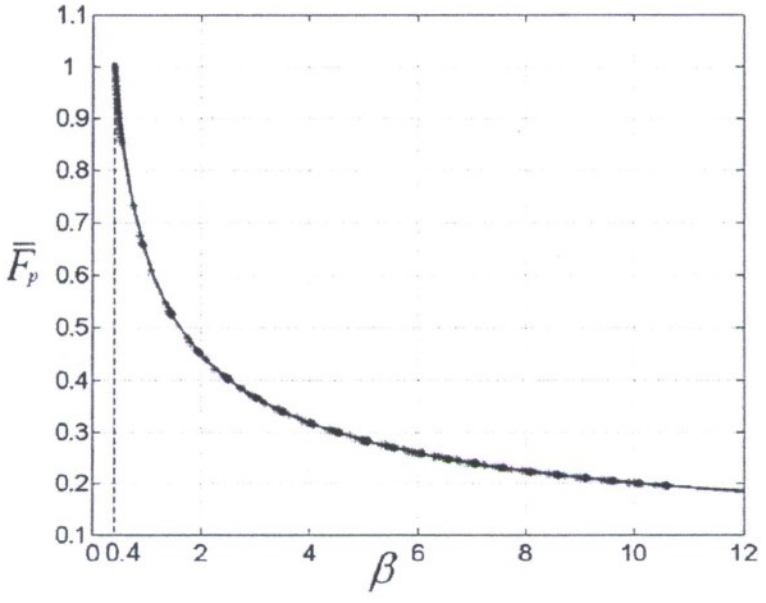

Figure 1: Normalized pull-off force for varying β. The symbols are numerical finite element results and the solid line is given by Equation (1) (from [2])

The pull-off force in eq 1 is normalized by the pull-off force with a zero thickness substrate:

$$F_p = \bar{F}_p \pi a^2 \delta_c = \frac{2}{\sqrt{\beta}} a^2 k \delta_c , \tag{8}$$

where δ_c is the critical extension of a single fiber at pull-off. This is where the single fiber model is incorporated into this soft adhesion model. As done previously, single fiber adhesion pull-off force P_f was initially modeled as a flat punch contact using Johnson-Kendall-Roberts theory[3]

$$\delta_c = \frac{P_f}{k_f} . \tag{9}$$

$$P_f = \sqrt{6\pi a_f^3 K w_f} , \tag{10}$$

$$K = \frac{4}{3}\left(\frac{1-\nu_s^2}{E_s} + \frac{1-\nu_f^2}{E_f}\right)^{-1} , \tag{11}$$

where w_f is the effective work of adhesion, a_f is the fiber radius, and K is the effective Young's modulus. E_s and E_f are the Young's moduli and ν_s and ν_f are the Poisson's ratios of the substrate and the fiber material, respectively. Combining Equations (8) and (9) gives

$$F_p = \frac{2}{\sqrt{\beta}} a^2 \rho P_f , \tag{12}$$

Interestingly, even though softer substrates result in lower adhesion, the equations suggest that softer fibers will increase adhesion. Although eq 10 indicates that the single fiber force will decrease for a softer fiber (assuming the work of adhesion is unchanged), the effect of the softer fibers on β outweighs it, as seen in Figure 2.

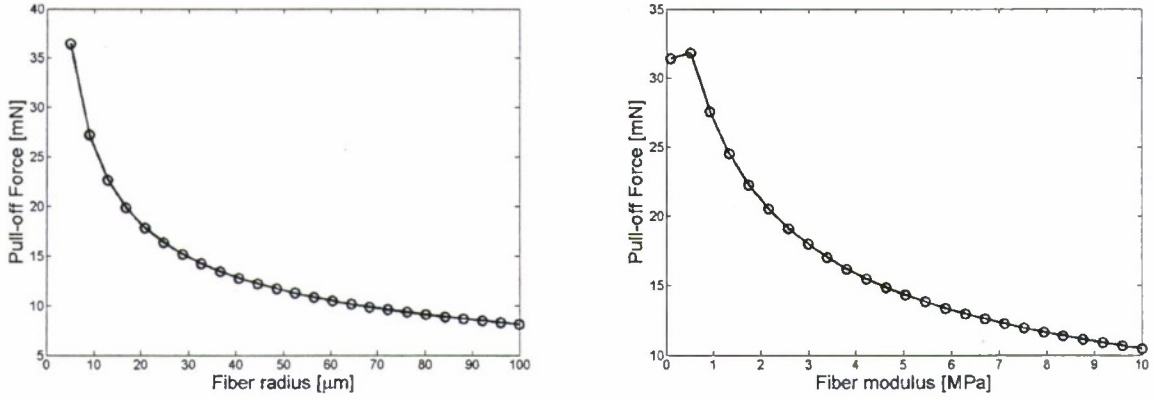

Figure 2: Model simulations examining the effect of changing the fiber radius and fiber material modulus. For both simulations, all other model parameters were held constant. For the fiber radius simulation, the overall area coverage of the fibers was held constant (as opposed to fiber spacing or number of fibers per unit area). In both cases, more compliant fibers result in greater adhesion.

3. ADHESIVE FABRICATION

3.1 Microfibers

The new model requires a circular area of fibers attached to a rigid cylindrical punch. To achieve this, small pegs with a radius of approximately 1 mm were cut out of an acrylic sheet with a laser cutter. The standard procedure for fabricating fibers was followed up to the point where uncured polyurethane is poured into the pink silicone rubber mold. Instead of filling the entire mold to create a large array of fibers with a backing layer, a small droplet of polyurethane is deposited on the mold, on top of which the acrylic peg is then placed. The mold is then placed in a vacuum chamber to ensure the polyurethane fills the holes in the mold. Capillary forces pull the acrylic peg towards the mold such that when the polyurethane is cured and the peg is pulled off of the silicone rubber, the backing layer between the acrylic and the fibers is very thin (on the order of 100 μm). The procedure for adding spatulate tips to the fibers can be performed as usual with the pegs.

To test against the model, two fiber geometries were chosen for comparison: the 50 μm diameter fibers with 70 μm edge-to-edge spacing that were found to perform the best in the previous two phases; and 30 μm diameter fibers with 50 μm diameter edge-to-edge spacing. The 50 μm fibers ended up with 100 μm diameter spatulate tips, whereas the 30 μm fibers had 50 μm diameter spatulate tips. All fibers were approximately 100 μm in length. Both geometries were fabricated out of two different types of polyurethane, again for comparison with the model: ST-1060 (Young's modulus of 2.9 MPa) and a harder ST-1087 (Young's modulus of 9.8 MPa). Microscope images of the fabricated fibers can be seen in Figure 3. The fabrication results are not perfect, but should be sufficient for testing purposes.

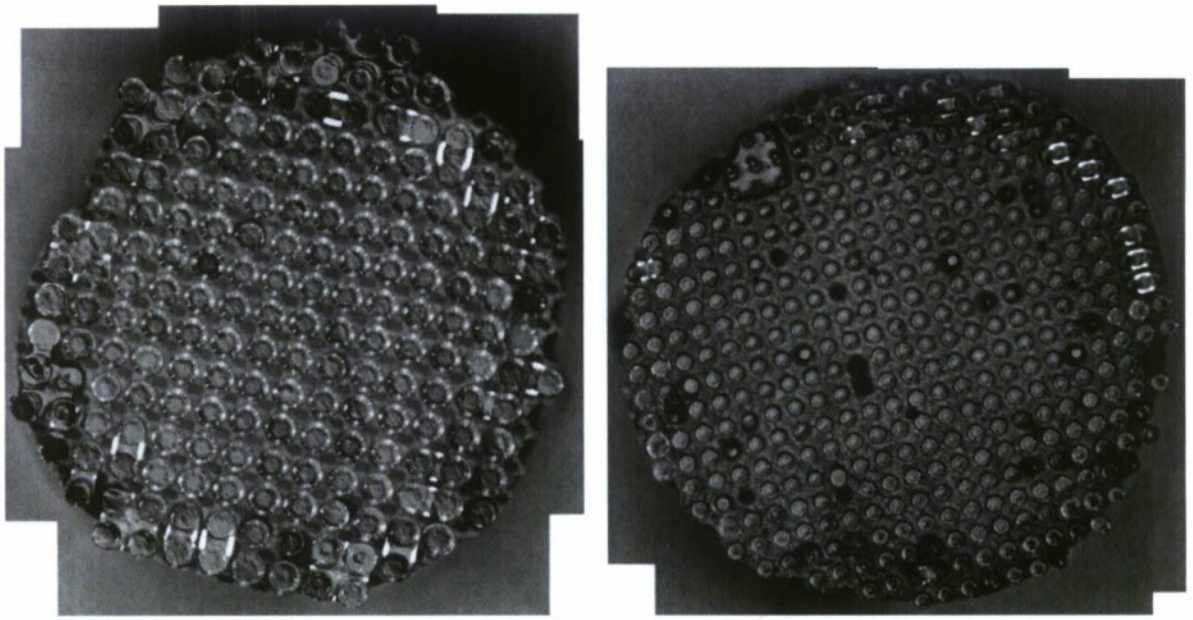

Figure 3: Top view microscope images of fibers with spatulate tips fabricated on acrylic pegs. On the left are 50 μm diameter fibers with 100 μm diameter spatulate tips. On the right are 30 μm diameter fibers with 50 μm diameter spatulate tips.

3.2 Substrates

First, a series of smooth substrates of varying softness and thicknesses were prepared by molding different polyurethanes against smooth plastic surfaces. The three materials chosen were, in order of increasing Young's modulus, F-15 (200 kPa), ST-1060 (2.9 MPa), and ST-1087 (9.8 MPa). The thicknesses fabricated were 0.7, 1.5, 3.0, and 5.5 mm. Because of bonding between like materials, the ST-1060 fibers could not be tested on the ST-1060 substrates. Likewise, the ST-1087 fibers could not be tested on the ST-1087 substrates.

The softest polyurethane (F-15) was then molded to create textured surfaces that more closely approximate the texture of human skin. Aluminum plates were roughed up in various ways and their roughnesses characterized with an atomic force microscope (AFM). Negative molds of these plates were created with silicone rubber, and the F-15 polyurethane then poured into the silicone rubber to create a soft, textured surface of known roughness. The two roughnesses chosen for this work were a nearly smooth 118 nm root-mean-square (RMS) and a much more textured 1.39 μm RMS.

For the final tests, a thin water layer was desired to mimic a sweat film that can accumulate on the face. However, polyurethane is hydrophobic, so some surface treatment is necessary to achieve this. A standard method for increasing hydrophilicity is oxygen plasma treatment. By exposing the polyurethane to a corona discharge, the surface energy will be increased, resulting in a greater attraction between the surface and water. The textured polyurethane surfaces described in the last paragraph were exposed to a corona discharge for 5 min. Unfortunately, the oxygen plasma melted the polyurethane, such that the final surface roughness was unknown. However, a thin water film was achieved.

4. TENSILE ADHESION TESTS

4.1 Tensile Adhesion Measurement Setup

The adhesion measurements were performed with a modified version of the sphere-flat tensile adhesion measurement system used in Phase II.[1] As the measurement requires alignment of two flat surfaces (the peg and the substrate), a slight change in the procedure was necessary. The acrylic peg was placed fibers down on the soft substrate. In this manner, the two flat surfaces are aligned perfectly through gravity. Attached to the load cell is a small aluminum cylinder 1/4 in. in diameter. A small droplet of quick-setting superglue is placed on top of the acrylic peg, and the load cell is lowered with the mechanical stage until the aluminum cylinder just makes contact with the peg. When the glue sets, the two surfaces will be in perfect alignment, and the standard adhesion tests can be performed. For all of the experiments performed in this section, the speed of the stage was set to 10 μm/s. A drawing of the setup after the peg has been glued is shown in Figure 4.

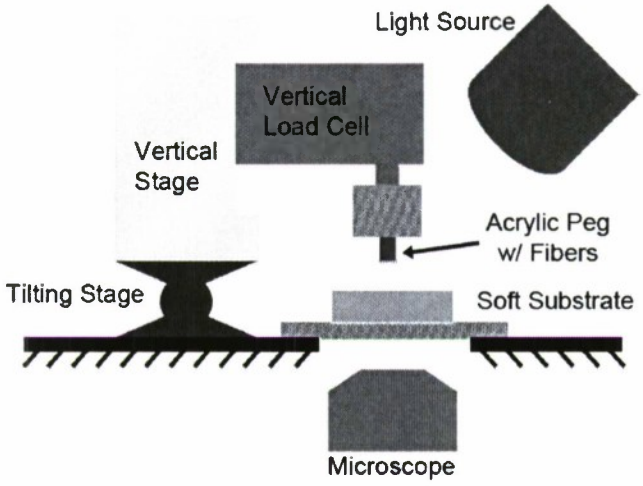

Figure 4: Sketch of the measurement setup used to perform flat-flat tensile adhesion tests with fibers fabricated on the end of an acrylic peg. The tilting stage is used to ensure that the attached linear stage and load cell are oriented vertically.

4.2 Soft Substrate Adhesion Results and Discussion

4.2.1 Smooth Soft Substrates

The results of the adhesion tests on smooth substrates of various thicknesses are shown in Figure 5. Adhesion to smooth surfaces is not dependent on preload, so the experiments were performed with a high preload. For the 50 μm diameter fibers, this preload was 100 mN. This preload would buckle the 30 μm diameter fibers, so the experiments with the smaller fibers were performed with a 50 mN preload. For each plot, the same fiber sample was used for every experimental data point. Each marker corresponds to five measurements. The model tends to underestimate the measured adhesion, but at least on the smooth F-15,

the model correctly captures the trends. For the harder polyurethane substrates, the high adhesion values were predicted by the model, but the experimental values were somewhat erratic. This can be attributed to fiber collapse problems, especially for the smaller diameter fibers. When the fibers release from the substrate, they snap back due to their large extension. When this happens, neighboring fibers may stick together, rendering them incapable of contributing to the next adhesion experiment. This effect is more pronounced for softer fibers (smaller diameter or softer material) and was observed occurring during testing of the ST-1060 30 μm diameter fibers. Therefore, even though the model suggests more compliant fibers are better, there is a constraint when durability/repeatability is taken under consideration. With the current length of the fabricated fibers, the 30 μm diameter fibers are too prone to collapsing problems to be useful.

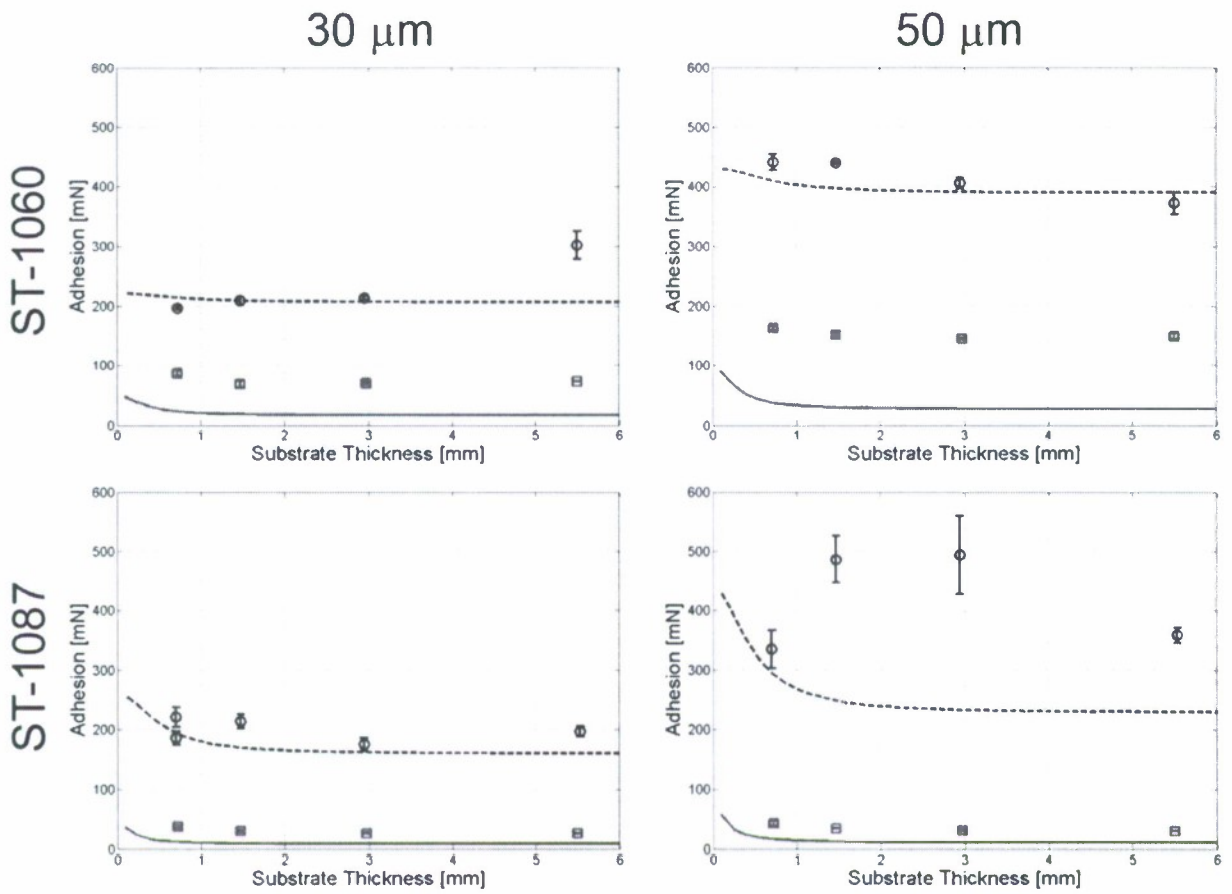

Figure 5: Compiled results of the smooth soft substrate adhesion tests. The columns denote different fiber radii. The rows denote different fiber materials. Markers represent experiment results; lines are model simulations. Solid lines and square markers are for the F-15 polyurethane substrate. Dashed lines and circular markers are for the harder polyurethane substrate (ST-1087 for ST-1060 fibers, ST-1060 for ST-1087 fibers).

The fact that the model underestimates the measured adhesion values is to be expected. The model uses a flat punch approximation for the adhesion of a single fiber, but this is known to be a bad assumption for a spatulate tip .[4] The interface between the fiber tip and substrate fails when any portion reaches a critical stress. A crack forms at this portion and propagates through the interface, causing the entire interface to fail quickly. The pull-off force is

then an integration of the stress over the entire interface. Clearly, the maximum pull-off force occurs when the stress is constant over the entire interface. For a flat punch, the stress profile has a minimum in the center of the fiber, and increases monotonically towards the edge. Typically the stress increases rapidly very close to the edge, resulting in a pull-off force much less than the maximum possible. However, the spatulate tip is much more compliant towards the edge, which provides some stress relief. As a result, the stress profile is more even, with a maximum in the center. Therefore, the pull-off force for a spatulate tip of a given radius will be much greater than the pull-off force of a flat punch of the same radius.

4.2.2 Textured Soft Substrates

The results of the adhesion tests on textured substrates of different roughnesses are shown in Figure 6. For each plot, the same fiber sample was used for every experimental data point. Due to the fiber collapse issues noted in the previous section, fresh samples were used. Each marker corresponds to five measurements. The lines corresponding to smooth results on each plot were taken from the steady state values in the previous section. Because of the different samples, some of the 118 nm RMS measurements showed greater adhesion than the smooth results. However, it is clear that for the rougher 1.39 μm RMS polyurethane substrate, there was a drastic reduction in adhesion for all fibers.

It is possible to adjust the model to take into account the substrate roughness. It has been shown for elastic solids that if certain roughness parameters of the surfaces are known, their adhesion can be adjusted by the simple multiplication of a coefficient.[5] The effect is analogous to a reduction in the work of adhesion between the two materials. Recent work in this lab has shown that this applies for fibrillar adhesion as well.

4.2.3 Water Covered Soft Textured Substrates

The results of the adhesion tests on textured substrates with a thin layer of water are shown in Figure 7. Based on previous results, only the 50 μm diameter, ST-1060 fibers with spatulate tips were used. The same fiber sample was used for every experimental data point, and each point corresponds to five measurements.

The effect of the corona discharge can be clearly seen, as the dry adhesion values increased after the surface treatment. In the case of the 1.39 μm RMS roughness polyurethane, a significant amount of the adhesion increase can be attributed to the melting of the polyurethane smoothing out the asperities. As expected, the thin water layer decreased the adhesion between the fibers and the substrate. However, the important result is that the measured adhesion was repeatable. Previous results suggested that the fibers would lose all adhesion when inundated with water.

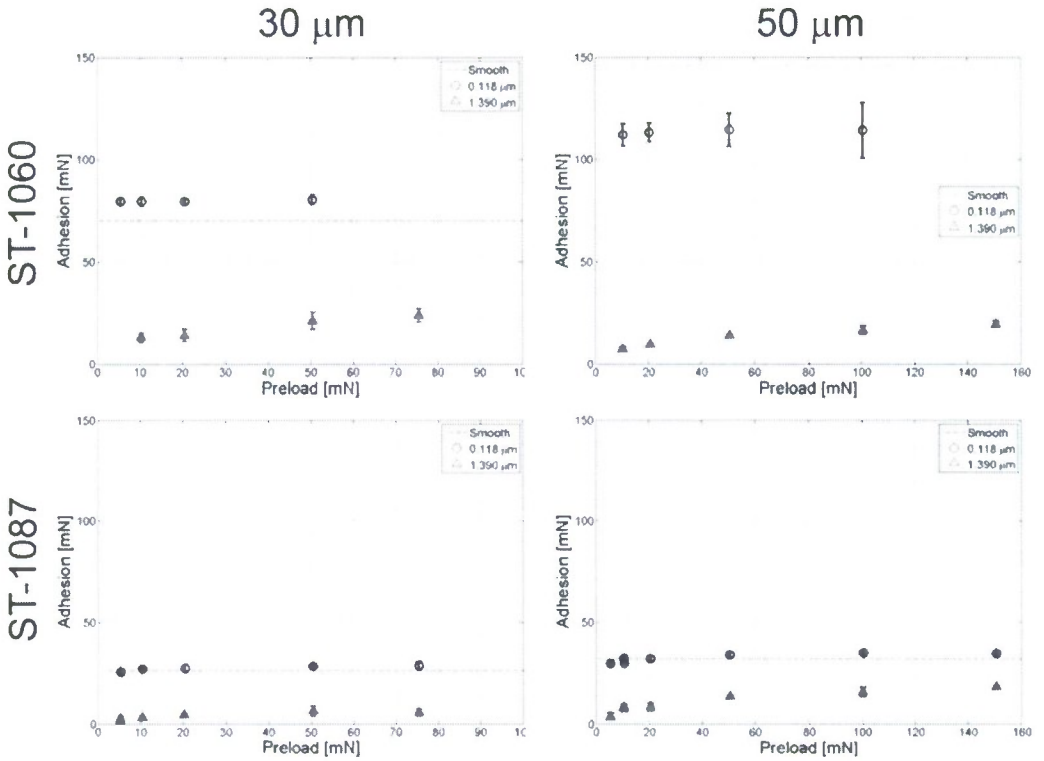

Figure 6: Compiled results of the textured soft substrate adhesion tests. The columns denote different fiber radii. The rows denote different fiber materials. Circles are for the smoother 0.118 µm RMS substrate, triangles for the rougher 1.390 µm RMS substrate. The dashed lines represent the smooth substrate results for comparison.

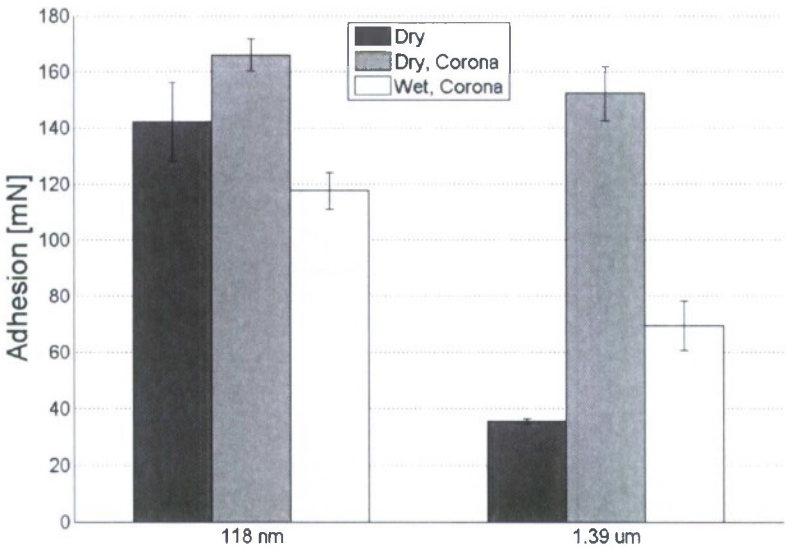

Figure 7: Results of adhesion tests on textured soft substrates with a thin water layer. To achieve a thin water layer, the substrates were exposed to a corona discharge for 5 min, altering the surface properties considerably (creating a hydrophilic surface for some duration).

5. FRICTION TESTS ON SOFT SUBSTRATES

An important characteristic that has only been briefly touched on previously is the friction performance of these adhesives. Although it is possible to maintain a good seal during lateral slipping, it is desirable to prevent such shear motions as it becomes more likely for the seal to fail under these conditions.

A simple alteration to the tensile adhesion setup allowed for descriptive friction measurements. The substrate, which was previously placed on the stage of the inverted microscope, is instead placed on a glass slide attached to a second load cell that measures force in the lateral direction. The glass slide is positioned over the objective of the inverted microscope to allow for viewing of the interaction between the fibers and the substrate during the experiment. The second load cell is attached to a motorized stage also oriented in the lateral direction. After performing the same procedure to align the peg with the flat substrate, the friction test can then be run as follows: first, the stage is lowered down into the substrate until a specified normal force is reached; then, the vertical position is held constant, while the substrate is dragged in the lateral direction. During the entire process, normal and lateral forces are measured. For the experiments performed for this report, the dragging speed was set to 10 μm/s.

The 50 μm diameter, ST-1060 fibers with spatulate tips were friction tested on the two textured F-15 polyurethane substrates. Four different preloads were used for comparison. The results are compiled in Figure 8. An examination of the results on the smoother 118 nm RMS F-15 is instructive. As the lateral motion is initiated, the lateral force (gray line) increases, whereas the normal force (black line) decreases. As the video confirms, this corresponds to the fibers adhering to the substrate. As the fibers are pulled to the side, they begin to stretch until their maximum adhesion is reached where they separate from the substrate. This separation occurs at the maximum of the lateral force curve. Because the lateral force arises from the adhesion of the fibers to the substrate, this type of friction is known as "adhesive friction." For smooth substrates where adhesion is independent of applied preload, the corresponding adhesive friction should likewise be independent of preload. Indeed, it can be seen in the graphs that the adhesive friction peaks are at approximately the same value across the entire range of tested preloads. After the fibers release, they remain bent over, and the edges of the fiber tips drag along the substrate. This friction regime, where the two surfaces merely rub against each other, is the standard Coulomb friction where the friction force is simply the preload multiplied by a coefficient of friction micron (in this case, $\mu \approx 1$).

The adhesive friction peak is not nearly as high on the 1.39 μm RMS F-15 substrate, as expected from the decreased adhesion. In fact, once the preload exceeds the maximum adhesive friction, this peak can be masked by the Coulomb friction.

These friction data show that even on textured soft substrates, optimal friction performance will result from adhesive friction. As adhesive performance is improved, a corresponding improvement in friction can be expected.

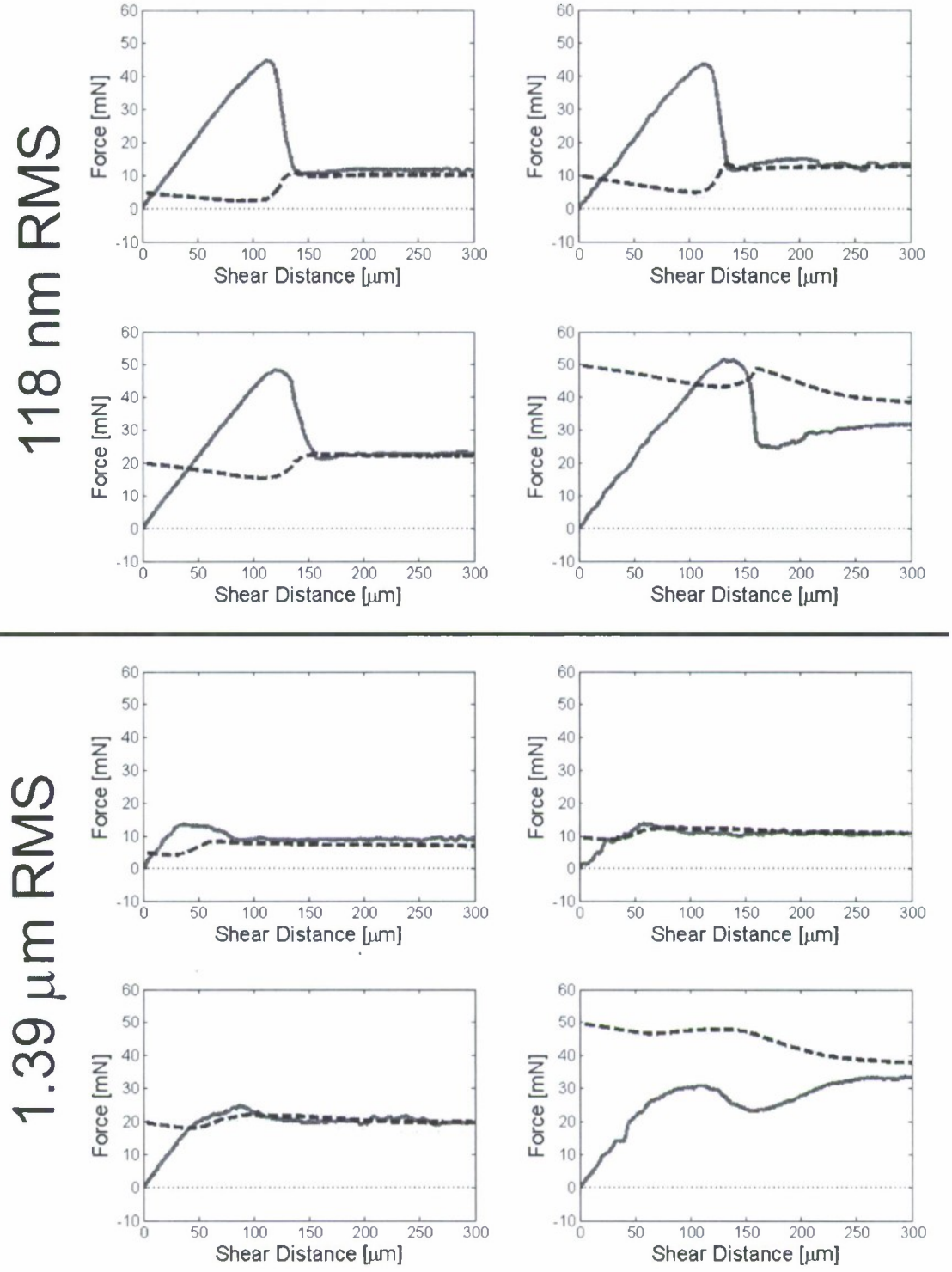

Figure 8: Results of friction tests on textured soft substrates. The dashed line is the average normal force over five experiments. The solid line is the average lateral force over five experiments. The top set of four graphs corresponds to four different preloads on 118 nm RMS F-15 polyurethane. The bottom set of four graphs corresponds to the four different preloads on 1.39 μm RMS F-15.

6. SEALING TESTS

The same vacuum assisted sealing setup used in Phases I and II[1] was used to evaluate the sealing performance of dry polyurethane adhesives on soft textured surfaces. Based on the previous adhesion tests, only the 50 μm diameter fibers with spatulate tips made out of ST-1060 polyurethane were used in the sealing experiments. The annulus shaped large scale fiber arrays used in the last two phases of this project were tested on the textured F-15 polyurethane substrates. Preloads up to between 40 mN and 10 N were used to attempt to maintain a seal with a leakage rate below 15 mL/min.

Even at the highest preload, the fibers by themselves were incapable of maintaining a sufficient seal on any textured surface, leaking at a rate an order of magnitude higher than the required specifications. However, when the fibers are encapsulated with a sealing structure as described in previous reports, a good seal can be achieved at even low preloads. At the lowest sustained preload of 40 mN, the encapsulated fibers had a leakage rate of about 5 mL/min on the rougher 1.39 μm RMS surface. At higher preloads, the leakage rate dropped well below 1 mL/min.

7. CONCLUSIONS

Building on the work done in previous phases of this project, a better understanding of adhesion and friction to soft, textured surfaces has been demonstrated. Models developed and experimentally verified for adhesion to soft, textured substrates reveal that the resulting adhesion is simply a fraction of the adhesion to a smooth, rigid substrate. The exact fraction depends on the fiber and substrate properties. The addition of a water layer further reduces the achievable adhesion. Furthermore, friction performance was shown to directly follow the adhesion performance of these spatulate-tipped fiber arrays.

A solid foundation has been built towards the development of a reliable fibrillar adhesive for use on human skin. Although the current adhesives are inadequate for the final application, there are many possible avenues to pursue to improve them. The fabricated adhesives are clearly not optimal; with the developed models, an optimal fiber configuration can be found (length, density, etc.) with the collapse constraint taken into account. Another promising line of research is the use of surface treatments (such as coatings) on the fibers to increase their adhesion to human skin.

LITERATURE CITED

1. Cheung, E.; Sitti, M. *Biologically Inspired Polymer Micro-Patterned Adhesives*; ECBC-CR-097; U.S. Army Edgewood Chemical Biological Center: Aberdeen Proving Ground, MD, 2008; UNCLASSIFIED Report (AD-A491 482).

2. Long, R.; Hui, C.-Y.; Kim, S.; Sitti, M. Modeling the Soft Backing Layer Thickness Effect on Adhesion of Elastic Microfiber Arrays. *J. Appl. Phys.* **2008**, *104:*4:044301.

3. Maugis, D. Contact, Adhesion and Rupture of Elastic Solids; Springer-Verlag: New York, 2000.

4. Spuskanyuk, A.V.; McMeeking, R.M.; Deshpande, V.S.; Arzt, E. The Effect of Shape on the Adhesion of Fibrillar Surfaces. *Acta Biomaterialia* **2008**, *4:*6, 1669–1676.

5. Persson, B.N.J.; Tosatti, E. The Effect of Surface Roughness on the Adhesion of Elastic Solids. *J. Chem. Phys.* **2001**, *115:*12, 5597–5610.